relatively long lifetimes to decomposition of ketene and methyl ketene molecules are not due to electronic multiplicity correlation rules. The lifetimes of these molecules can be likened to those of thermally activated molecules, the delay in both cases being due to migration of vibrational amplitude among several bonds of the molecule. On this basis, the lifetime of the photo-excited molecules behave as qualitatively predicted by eq. 13; the lifetimes decrease with total energy and increase with the complexity of the molecule.

CAMBRIDGE 38, MASS.

---

[CONTRIBUTION FROM THE RESEARCH AND DEVELOPMENT DIVISION, HUMBLE OIL & REFINING COMPANY]

# Reactions of Gaseous Ions. I. Methane and Ethylene

BY F. H. FIELD, J. L. FRANKLIN AND F. W. LAMPE

RECEIVED OCTOBER 1, 1956

At elevated pressures in a mass spectrometer ion source reactions occur between certain ions and the neutral species present. We have studied the various secondary ions formed in methane and ethylene at elevated pressures and have determined the reactions by which they are formed and the rates of these reactions. The rates are all extremely fast. The reaction rates have been treated by classical collision theory and it has been shown that to a fair approximation the cross-sections and reaction rate constants can be predicted from a simple balance of rotational and polarization forces.

## Introduction

Secondary processes in mass spectrometers were first observed by early workers in the field[1] but were treated, for the most part, as nuisances due to experimental difficulties that had to be overcome in the development of analytical mass spectrometry. In recent years, however, a number of studies of secondary processes have been reported[2] which are of considerable interest because of the information afforded concerning the gaseous reactions of ions with molecules. Tal'roze and Lyubimova[3] reported the formation of $CH_5^+$ in methane. Stevenson and Schissler[4] published specific reaction rates for the formation of $CD_5^+$ in deuterated methane, $D_3^+$ in deuterium, and for the reactions of $A^+$ with $H_2$, $D_2$ and HD. In a recent note Schissler and Stevenson[5] have reported many more ion–molecule reactions included in which are reactions forming $C_2H_5^+$ and $C_2D_5^+$ in methane and deuterated methane, respectively, and $C_2H_5^+$, $C_3H_3^+$ and $C_3H_5^+$ in ethylene. These reactions were reported to exhibit cross-sections that decreased to zero at finite values of ion-energy and small negative temperature coefficients.

This paper comprises a detailed study of the ion–molecule reactions taking place in methane and ethylene when these compounds are subjected to ionization by electron impact in a mass spectrometer.

## Theoretical

Consider the reaction of a primary ion with a neutral molecule to consist of the formation of a transition-state ion which then decomposes unimolecularly to various product ions and neutral fragments. That is

$$P^+ + M \xrightarrow{k_1} PM^+ \qquad (R1)$$

$$PM^+ \xrightarrow{k_{S_j^+}} S^+{}_j + F_j \qquad (R2)$$

where there will be a set of the above reactions for each primary ion that reacts with neutral molecules. If the time of decomposition of the transition-state ion is short compared with ionic residence times in the ionization chamber, the number of secondary ions of the jth type that are formed will be

$$n_{S_j^+} = \frac{k_{S_j^+}}{\sum_j k_{S_j^+}} n_{PM^+} \qquad (1)$$

where the $n$'s are the number of ions of the various kinds formed per unit time. Since the primary ions are formed in the electron beam at a constant rate, in the following for the sake of simplicity we shall in general refer to the $n$'s as the number of ions formed, the rate aspect of the process to be kept in mind at all times. The number of transition-state ions formed is equal to the product of the number of primary ions formed, the number of collisions made by one primary ion with neutral molecules during its ionization chamber residence time, and the collision efficiency or

$$n_{PM^+} = fQ[M]n^0{}_{P^+} \qquad (2)$$

where

$n^0{}_{P^+}$ = number of primary ions formed
$f$ = collision efficiency for the formation of $PM^+$
$Q$ = total no. of collisions made by a single primary ion with neutral molecules at unit concn.
[M] = no. of molecules per unit volume

Combining (1) and (2) and introducing $\tau$, the time in which the primary ion makes collisions with neutrals (the primary ion residence time), gives

$$n_{S_j^+} = \frac{k_{S_j^+}}{\sum_j k_{S_j^+}} n^0{}_{P^+} f \frac{Q}{\tau_{P^+}} [M]\tau_{P^+} \qquad (3)$$

$Q/\tau_{P^+}$ is the time-average collision rate, and the product of this quantity and the collision efficiency is the rate constant for the formation of the transition-state ion. Recognizing this and rearranging (3) gives

$$\frac{n_{S_j^+}}{n^0{}_{P^+}} = \frac{k_{S_j^+}}{\sum_j k_{S_j^+}} k_1 [M]\tau_{P^+} \qquad (4)$$

The number of primary ions formed will be propor-

(1) H. D. Smyth, *Rev. Mod. Phys.*, **3**, 347 (1931).
(2) For a complete review see F. H. Field and J. L. Franklin, "Electron Impact Phenomena and the Properties of Gaseous Ions," Academic Press, New York, N. Y., in press.
(3) V. L. Tal'roze and A. K. Lyubimova, *Doklady Akad. Nauk. S.S.S.R.*, **86**, 909 (1952).
(4) D. P. Stevenson and D. O. Schissler, *J. Chem. Phys.*, **23**, 1353 (1955).
(5) D. O. Schissler and D. P. Stevenson, *ibid.*, **24**, 926 (1956).

tional to the number of primary ions collected plus the number of secondary ions (derived from the primary ions) collected. Thus, if we assume equal collection efficiencies for all ions we can write (remembering that the $n$'s are really numbers of ions per unit time)

$$\frac{I_{S_j^+}}{I_{P^+} + \sum_j I_{S_j^+}} = \frac{k_{S_j^+}}{\sum_j k_{S_j^+}} k_1 [M] \tau_{P^+} \quad (5)$$

where the $I$'s are the observed ion-currents. In addition, it is easily shown that

$$\frac{I_{S_j^+}}{I_{S_k^+}} = \frac{k_{S_j^+}}{k_{S_k^+}} \quad (5a)$$

To determine specific reaction rates from experimental measurements it is necessary to calculate the average residence time of the primary ions in the ionization chamber. In these calculations an idealized model of the ionization chamber is used, in that we ignore the effects of: (1) the magnetic field in the ionization chamber, (2) potential penetrations through the various ionization chamber orifices, (3) space charge effects, and (4) surface charge effects. The electron beam is assumed to be of infinitesimal thickness and the potential gradient in the ionization chamber (due to the ion-repeller) is taken as uniform.

Consider the primary ion to be formed in the electron beam at a distance $d_0$ from the ion-exit slit and at the moment of its formation to be moving with average thermal velocity in a direction making an angle $\phi$ with the perpendicular directed from the electron beam to the slit. It easily can be shown from the laws of motion that the residence time, $\tau$, of an ion reaching the ion-exit slit is given by

$$\tau = \frac{1}{A}\sqrt{2Ad_0 + B^2\cos^2\phi} - \frac{B}{A}\cos\phi \quad (6)$$

where

$A = eV/m$
$B = \sqrt{8kT/\pi m}$
$e$ = electronic charge
$V$ = voltage gradient in the ionization chamber
$m$ = mass of the ion

Since all values of $\phi$ are equally probable, the average ion residence time is obtained by integration as

$$\bar{\tau} = \frac{1}{4\pi}\int_0^\pi \tau(2\pi \sin\phi)\, d\phi \quad (7a)$$

or

$$\bar{\tau} = \frac{1}{2A}\sqrt{B^2 + 2Ad_0} + \frac{d_0}{2B}\ln\frac{\sqrt{B^2 + 2Ad_0} + B}{\sqrt{B^2 + 2Ad_0} - B} \quad (7b)$$

This equation does not apply accurately at ionization chamber voltage gradients less than about 1 volt/cm. since at lower fields some of the ions will be lost by striking the ion repeller.

The reaction rate constant $k_1$ can be evaluated from the observed ion currents by the use of equations 5, 5a and 7b.

By means of the following analysis the observed ion currents can be used to determine the cross section for the reaction $P^+ + M \rightarrow PM^+$. By combining equations 1 and 2 and converting to currents we obtain

$$\frac{n_{S_j^+}}{n_{P^+}} = \frac{I_{S_j^+}}{I_{P^+} + \sum I_{S^+}} = \frac{k_{S_j^+}}{\sum k_{S^+}} fQ[M] \quad (8a)$$

$Q$, the total number of collisions made by a single primary ion with neutral molecules at unit concentration can be written

$$Q = \sigma Q' \quad (8b)$$

where

$Q'$ = total no. of collisions made by a primary ion during its ionization chamber lifetime with neutral molecules at unit concn. taking the collision cross-section to be unity
$\sigma$ = collision cross-section for a primary ion and neutral molecule

Substituting (8b) in (8a) gives

$$\frac{I_{S_j^+}}{I_{P^+} + \sum_j I_{S_j^+}} = \frac{k_{S_j^+}}{\sum_j \Sigma_{S_j^+}} k f\sigma Q'[M] \quad (8c)$$

For a reaction with no activation energy, $f\sigma$ constitutes the reaction cross-section. Equation 8c permits the evaluation of this quantity from experimental measurements if $Q'$ is known.

To obtain an expression for $Q'$, we again consider the primary ion to be formed in the electron beam at a distance $d_0$ from the slit and at the moment of its formation to be moving with average thermal velocity in a direction making an angle $\phi$ with the perpendicular directed from the electron beam to the side of the chamber containing the slit. We assume that the number of ions of each type emerging from the slit is proportional to the number in the ionization chamber. If this is true the position of the ion, at the instant of its formation, along an axis parallel to the electron beam is arbitrary and we take this coördinate to be zero. The velocity of any ion at time $t$ after its formation can then be shown to be

$$v = \sqrt{B^2 + A^2t^2 + 2ABt\cos\phi} \quad (9)$$

where the symbols are as defined previously. The average ion velocity is obtained by integration over all directions as before and is

$$\bar{v}_1 = \left(B + \frac{A^2t^2}{3B}\right) \quad (10)$$

for the region in which $B > At$.

$$\bar{v}_2 = \left(At + \frac{B^2}{3At}\right) \quad (11)$$

for the region in which $At > B$.

Similarly, the average relative velocity of two species $\alpha$ and $\beta$ moving at different velocities is

$$\bar{\xi}_1 = \left(v_\alpha + \frac{v_\beta^2}{3v_\alpha}\right) \text{ for } v_\alpha > v_\beta \quad (12)$$

$$\bar{\xi}_2 = \left(v_\beta = \frac{v_\alpha^2}{3v_\beta}\right) \text{ for } v_\beta > v_\alpha \quad (13)$$

where $\xi$ denotes relative velocity.

Substituting (10) and (11) for the ion velocity, $v_\beta$, and $B$ for the average thermal velocity, $v_\alpha$, of the neutral molecules into (12) and (13) results in

$$\xi_1 = \frac{1}{3}\left(4B + \frac{2A^2t^2}{3B} + \frac{A^4t^4}{9B^3}\right) \text{ for } At < B \quad (14)$$

$$\xi_2 = \frac{1}{3}\left(3At + \frac{B^2}{At} + \frac{3AtB^2}{3A^2t^2 + B^2}\right) \text{ for } At > B \quad (15)$$

Therefore, for unit cross-section, the total number of collisions made by one primary ion with neutral molecules at unit concentration during the time $\bar{\tau}$ is

$$Q' = \int_0^{B/A} \xi_1\, dt + \int_{B/A}^{\tau} \xi_2\, dt \qquad (16)$$

where $B/A$ is the time at which the ion and molecule velocities are equal. Integration of (16) gives

$$Q' = \frac{A\bar{\tau}^2}{2} + \frac{B^2}{A}\left[\frac{247}{382} + \frac{1}{3}\ln\frac{1A\bar{\tau}}{\sqrt{B^2+3A^2\bar{\tau}^2}}\right] \qquad (17)$$

where $\bar{\tau}$ is given by (7b).

In the above derivation it was assumed the neutral molecules were all moving with average thermal velocity. Actually there exists a distribution of velocities. However, it has been shown[6] that consideration of this distribution leads to a small difference in relative velocities that is well within our experimental error.

## Experimental

Three types of measurements were made: (1) the variation of ion intensities with pressure (pressure studies), (2) the variation of ion intensities with ion repeller voltage (repeller studies), and (3) the appearance potentials of various ions. The first two types of measurements were made with a slightly modified Consolidated Electrodynamics Corp. (CEC) Model 21-620 cycloidal focussing mass spectrometer. The appearance potential measurements were made with a Westinghouse Type LV mass spectrometer.

The pertinent dimensions and operating characteristics of the CEC instrument are as follows. The distance between the ion repeller electrode and the ion exit slit is 1.0 mm., and the electron beam (thickness = 0.17 mm.) passes midway between the two. The length of the repeller electrode in the direction of the electron beam is 5.63 mm. The instrument as received from the manufacturer was modified by by-passing the pressure sensitive filament protection circuit and by altering the ion repeller circuit to permit the application of constant, predetermined repeller voltage. It is not provided with an adjustment for the electron accelerating voltage, and consequently all measurements were made at the manufacturer's pre-set value of about 75 volts. Similarly, no control over the ionization chamber temperature is provided (although the temperature can be measured), and temperature variations of 20–25° occurred from one experiment to another and even in the course of a single experiment. The actual value of the temperature may be taken as 150 ± 10°. The electron current was maintained at 2 $\mu$amp.

The methane and ethylene were of Phillips reagent grade, and they were condensed in liquid nitrogen and subjected to a bulb-to-bulb distillation. A middle fraction constituting about half the material condensed was collected for the measurements.

**Pressure Studies.**—The pressure studies involved the determination of the mass spectra of methane and ethylene at different values of the reservoir pressure. In the CEC mass spectrometer secondary ions begin to be formed in detectable amounts at a reservoir pressure of about 1 mm. In most of the experiments the reservoir pressure was varied between 1 and 30 mm. in steps of 2–5 mm. The reservoir pressure was determined by a small mercury manometer read with a cathetometer, and values obtained in this way were reproducible to 0.1 mm. In all pressure studies the repeller voltage was maintained at 1.0 volt, an arbitrarily selected value.

The quantitative interpretation of the results requires a knowledge of the pressure in the ionization chamber. To determine this quantity as a function of the more easily measured reservoir pressure, the ion repeller of the mass spectrometer was biased negatively with respect to the ionization chamber and the collected ion current measured with an RCA millimicroammeter. The repeller currents ($I_i$) for various reservoir pressures ($p_r$) were determined for argon and neon, and plots of $I_i/p_r$ against $p_r$ were constructed. For reservoir pressures up to about 4 mm. $I_i/p_r$ remained constant with pressure and then increased. From this behavior and from a rough comparison of the atomic mean free paths with the known diameter of the gas leak into the ionization chamber (1 $\mu$), we conclude that for relatively low molecular weight gases at reservoir pressures up to about 4 mm. the gas flow through the leak is molecular in character, but above this pressure mass flow occurs. In the region where molecular flow occurs, the ionization chamber atom concentration ($N_i$) can be expressed as $N_i = \gamma p_r$, and substituting in the relation $I_i/I_e = N_i Q_i l$ we get $\gamma = I_i/I_e Q_i l p_r$ ($I_e$ = electron current, $Q_i$ = total cross-section for ionization, and $l$ = length of the repeller). From this equation, values of $Q_i$ obtained from the data tabulated by Massey and Burhop,[7] and our experimental currents we find $\gamma_{Ne} = 7.7 \times 10^{12}$ and $\gamma_A = 7.3 \times 10^{12}$. These are equal to within experimental error, as is to be expected theoretically.

To establish the total cross-section for ionization for methane and ethylene it is assumed that in the molecular flow range of pressures the average of the values of $\gamma$ for argon and neon can be applied to methane and ethylene. Then the $Q_i$ values for these substances can be calculated from the observed currents in this pressure range. Knowing the $Q_i$ values the ionization chamber concentration corresponding to any reservoir pressure can be calculated from the observed currents.

The $Q_i$ values obtained are $Q_i(CH_4) = 4.8_3 \times 10^{-16}$ cm.$^2$ and $Q_i(C_2H_4) = 6.9_2 \times 10^{-16}$ cm.$^2$. Recently Otvos and Stevenson[8] have determined the relative total ionization cross-sections for a number of compounds, and from their data one calculates that $Q_i(C_2H_4)/Q_i(CH_4) = 1.55$. Our value for this ratio is 1.43, in satisfactory agreement. However, from Otvos and Stevenson, $Q_i(CH_4)/Q_i(Ne) = 4.28$, whereas our value is 7.75. Partially as a consequence of this discrepancy, we determined the total ionization cross-section of acetylene, obtaining the value $5.6_0 \times 10^{-16}$ cm$^2$. This agrees reasonably well with the value of $4.98 \times 10^{-16}$ cm.$^2$ quoted by Massey and Burhop. Unfortunately, Otvos and Stevenson do not give a value for the total ionization cross-section for acetylene by low energy electrons. However, their relative value for ethylene can be converted to an absolute value of $4.13 \times 10^{-16}$ cm.$^2$ using the Massey and Burhop value for $Q_i(Ne)$, and this ethylene value is appreciably lower than both our acetylene value and that given by Massey and Burhop. This seems quite suspicious, and consequently we have used our values of the methane and ethylene cross-sections in the determination of the ionization chamber concentrations.

An example of the variation of the intensities of primary and secondary ions as a function of the ionization chamber molecular concentrations, $N_i$, is given in Fig. 1. We think that the observed deviations from first- and second-order behavior are to be attributed to scattering of the ion beam in the analyzer and, if this be true, the intensity variation of $CH_4^+$, for example, should be represented by the relations

$$I_{CH_4^+} = aN_i e^{-\sigma_s L N_a} \qquad (18a)$$

$$\log (I_{CH_4^+}/N_i) = -\sigma_s L N_a/2.303 + \log a \qquad (18b)$$

where $\sigma_s$ is the scattering cross-section, $L$ is the path length in the analyzer (taken to be 8.0 cm. in our instrument), and $N_i$ and $N_a$ the molecular concentrations in the ionization chamber and the analyzer, respectively. Since the experimental plot of log $(I_{CH_4^+}/N_i)$ against $N_a$ is approximately a straight line (a small amount of curvature exists), we conclude that indeed the form of the $CH_4^+$ curve in Fig. 1 is for practical purposes completely accounted for by scattering in the analyzer, and we infer that all observed deviations from expected first- or second-order behavior can be attributed to this source. The values of $N_a$ used in the plot of eq. 18b were calculated from pressures indicated by an ionization gage located on the envelope of the analyzer. The gage was not calibrated. From the mean slope of the plot we calculate that for the scattering of $CH_4^+$ in $CH_4$ in our instrument $\sigma_s = 4.0 \times 10^{-15}$ cm.$^2$.

To enable us to assess the extent to which scattering affects the values of the current ratios $I_s/(I_p + I_s)$ needed in the kinetic calculations, we have derived[9] an approximate expression for the scattering of an ion beam in the analyzer of a mass spectrometer. The scattering is assumed to re-

(6) L. B. Loeb, "The Kinetic Theory of Gases," McGraw-Hill Book Co., New York, N. Y., Ind. Ed. 1934, p. 96.

(7) H. S. W. Massey and E. H. S. Burhop, "Electronic and Ionic Impact Phenomena," Oxford Univ. Press, 1952, p. 38.

(8) J. W. Otvos and D. P. Stevenson, THIS JOURNAL, **78**, 546 (1956).

(9) Details of the derivation are available on request.

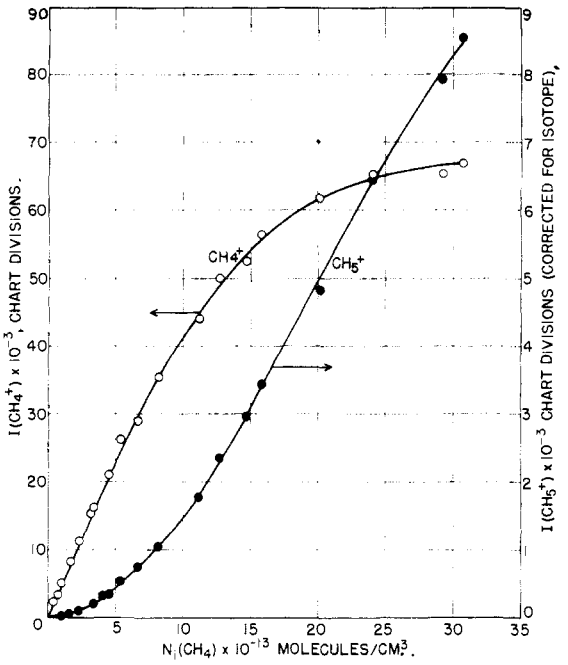


Fig. 1.—Primary and secondary ion currents against ion chamber concentration.

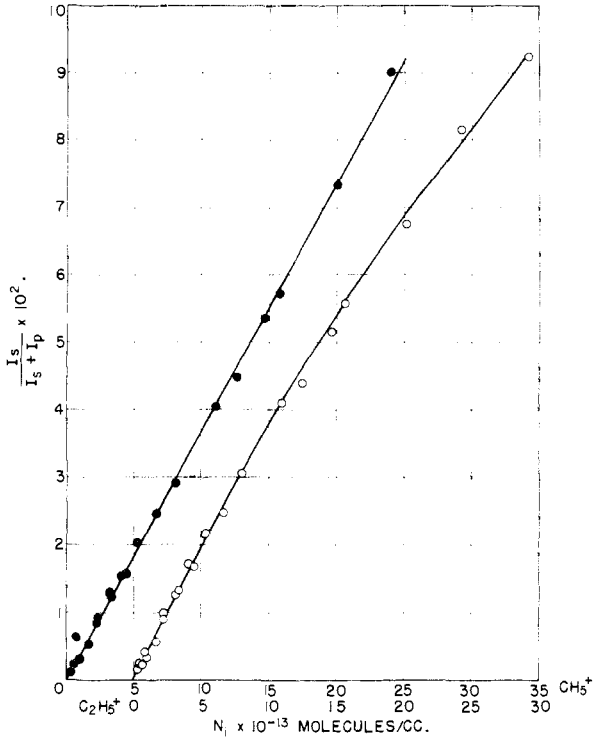


Fig. 2.—Typical curves of current ratios against ion chamber concentration.

sult solely from ion–molecule polarization interaction. The expression is

$$\sigma_s = \left(\frac{3\pi^3\alpha e L}{16 S_{eff}^2 V_{esu}}\right)^{1/2} = 41.8\left(\frac{\alpha e L}{S_{eff}^2 V_{pract.}}\right)^{1/2} \quad (19)$$

where

$\alpha$ = polarizability of the scattering gas
$e$ = electronic charge
$L$ = ion path length in analyzer in cm.
$V$ = ion accelerating voltage
$S_{eff}$ = av. distance from center of collector slit to edges of slit in cm.
$S_{eff} \cong \lambda/4$ where $\lambda$ = length of collector slit in cm.

For the scattering of $CH_4^+$ in $CH_4$ in our mass spectrometer we calculate from equation 19 that $\sigma_s = 2.0 \times 10^{-15}$ cm.$^2$, to be compared with the experimental value of $4.0 \times 10^{-15}$ cm.$^2$. The agreement is sufficiently satisfactory to lead us to believe that the theoretical dependence of $\sigma_s$ on $\alpha$ and $V$ is substantially correct, and thus we write $\sigma_s = b(\alpha/V)^{1/2}$. The constant $b$ is evaluated from the experimental value of $\sigma_s$, and the semi-empirical expression $\sigma_s = 1.45 \times 10^{-2}(\alpha/V)^{1/2}$ results.

For the formation of the $CH_5^+$ ion from methane we have the relation

$$\frac{I_{CH_5^+}}{I_{CH_4^+} + I_{CH_5^+}} \approx \frac{I_{CH_5^+}}{I_{CH_4^+}} \alpha N_i e^{-N_a L(\sigma_{CH_5^+} + \sigma_{CH_4^+})} \quad (20)$$

and using scattering cross-section values calculated from our semi-empirical expression we calculate that a graph of $I_{CH_5^+}/(I_{CH_4^+} + I_{CH_5^+})$ *versus* $N_i$ should not depart from linearity by as much as 10% until $N_a = 8.2 \times 10^{13}$ molecules/cc. Since the $N_a$ value corresponding to the highest $N_i$ value used in our experiments is $3.4 \times 10^{13}$, noticeable deviations of the current ratio from linearity should not be observed. As Fig. 2 shows, this prediction is correct. Similar calculations lead to the prediction that the graph of $I_{C_2H_5^+}/(I_{CH_5^+} + I_{C_2H_5^+})$ *vs.* $N_i$ should depart from linearity by 10% at $N_i = 4 \times 10^{13}$ molecules/cc., which is in approximate agreement with the behavior of the experimental graph given in Fig. 2. From these and similar results we feel that differential scattering effects are not important at ion source concentrations below about $N_i = 5 \times 10^{13}$ molecules/cc. The rate constants reported in this paper are calculated only from current ratios at concentrations below this value. Two other factors which will affect the accuracy of $I_s/(I_s + I_p)$ are (1) mass discrimination in the analyzer and (2) primary and secondary ions are formed in different regions of the ionization chamber. From discrimination information reported by Robinson[10] we estimate that the largest discrimination effect occurring in our experiments is 12%. The second factor might give rise to a difference in collection efficiency for the two types of ions, but we do not know the magnitude of the resulting error, if any, in the current ratio value.

**Repeller Studies.**—The repeller studies involved the determination of primary and secondary ion mass spectra at different values of the ion repeller voltage ($V_R$) at a known, essentially constant value of the reservoir pressure (about 5 mm.). Three types of variation of ion intensities with increasing repeller voltage are to be observed (Fig. 3). That for primary ions is illustrated by the plot of $I_{CH_4^+}$, while the two types observed for secondary ions are illustrated by the plots of $I_{CH_5^+}$ and $I_{C_2H_5^+}$. We are unable to explain these differences in behavior.

None the less, the forms of the intensity variations with repeller voltage can be used in interpreting the observed secondary spectrum of methane. By comparing Figs. 3 and 4 we conclude that the mass 29 and 17 ions are formed by one type of process, namely, a bimolecular gas phase ionic reaction, but that the mass 26, 27, 28 and 16 ions are formed by another type of process, namely, ionization by electron impact in the electron beam. Since the intensity of the mass 28 ion shows a first-order pressure dependence, it seems likely that it results from a small amount of impurity, probably $N_2$. However, the mass 26 and 27 intensities are second order in methane pressure and must be formed from methane by some kind of secondary reaction. The appearance potential of the mass 26 ion is 11.5 e.v., which, within the limits of experimental error, is equal to the ionization potential of acetylene. This suggests that the methane undergoes a bimolecular reaction (probably on the filament) to produce acetylene, which diffuses into the ionization chamber and undergoes ionization in the electron beam. The mass 27 ion probably is formed in the same way, although the observed appearance potential (12.1 e.v.) is of no help in elucidating the nature of the ion or the reaction by which it is formed.

(10) C. F. Robinson and L. C. Hall, *Rev. Sci. Instruments* **27**, 351 (1956).

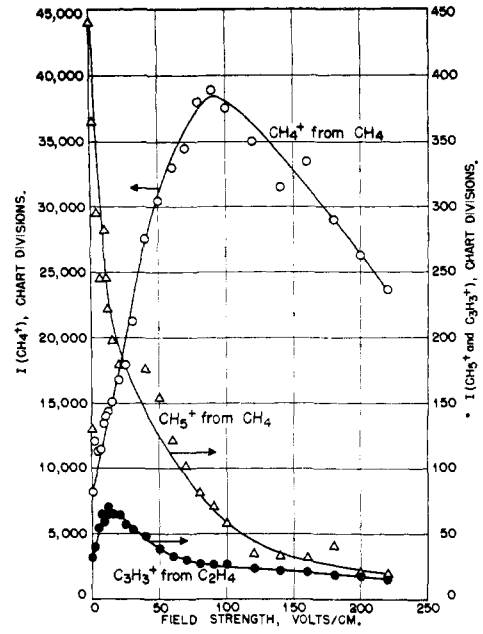


Fig. 3.—Primary and secondary ion currents against ionization chamber field strength.

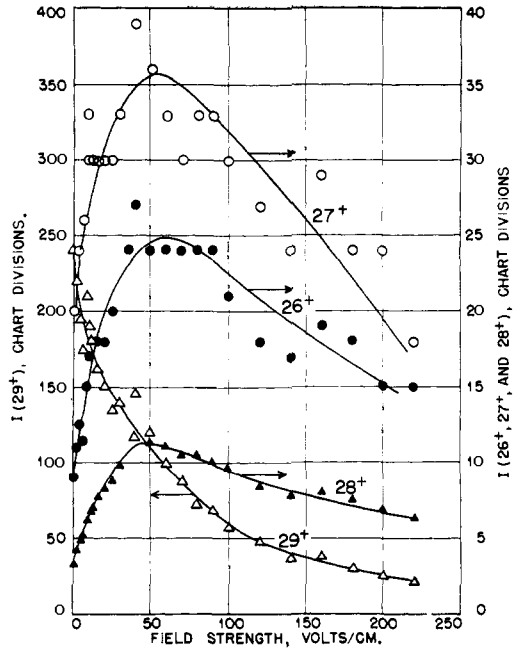


Fig. 4.—Plots of various ion currents from $CH_4$ against field strength.

Results obtained from repeller studies are subject to an uncertainty stemming from the possible variation in ion collection efficiency with repeller voltage. In addition, results at quite low values of $V_R$ (less than 1 volt) are particularly suspect because the conditions in the ion source at these low voltages are probably ill-defined. Potential penetrations through the ion exit slit and the electron beam slits, the potential depression in the electron beam, surface charges, etc., could cause the actual potential in the ionization chamber to be several tenths of a volt different from that calculated on the basis of only the applied repeller voltage.

An observation which may be related to problems of ion collection efficiency is that at values of $V_R > 2.5$ volts the observed intensity of the mass 29 ion from ethylene becomes smaller than the intensity of the $C^{12}C^{13}H_4^+$ ion as calculated from the observed intensity of the mass 28 ion. On the surface this means that the secondary ion contribution to the mass 29 intensity vanishes above $V_R = 2.5$ volts and is probably erroneous even below this value. We can offer no explanation for this behavior.

**Appearance Potential Measurements.**—Measurements of appearance potential were made in a Westinghouse Type LV mass spectrometer using the vanishing current technique. For most of the measurements $O_2$ introduced along with the material under investigation was used to calibrate the electron energy scale, but in a few measurements $CO_2$ was used. The methane or ethylene pressure in the gas reservoir was kept at about 10 mm., which gave about maximum secondary ion currents. Experimental difficulties prevented the determination of the ionization chamber pressure to which this reservoir pressure corresponds. The electron current was maintained at 3.0 $\mu$amp. and the ion repeller at 1.9 volts.

The ionization efficiency curves sometimes show breaks (discontinuities) which are attributable to the high pressures. These arise from two sources: (1) contributions to the ion current at a given mass from ions one or two mass units different as a result of scattering and (2) pyrolysis of the sample yielding products which upon ionization contribute to the ion current at the mass being investigated. The difficulty stemming from the first process can be circumvented by obtaining the appearance potentials by repeatedly scanning across the mass spectral region of interest at small increments of the ionizing voltage. The ion intensities free from scattered contributions can then be obtained by reading the peak heights from the means of the adjacent valleys. The occurrence of pyrolysis can be inferred from the form of the ionization efficiency curve, from the value of the lowest appearance potential, and from some knowledge of the chemical properties of the substance under investigation.

From the observed agreement of replicate determinations we estimate the uncertainty in the appearance potential values to be about 0.3 volt except for the values for the mass 50 and 51 ions from ethylene, which are probably uncertain to about 1 volt.

## Results[11]

Typical high pressure mass spectra (reservoir pressure = 10 mm.) of methane and ethylene are given in Table I. Table II contains the appearance potentials of the more important ions and the

TABLE I

HIGH PRESSURE MASS SPECTRA OF METHANE AND ETHYLENE ($P_r$ = 10 MM., $V_R$ = 1 V.)

| $CH_4$ | | $C_2H_4$ | |
|---|---|---|---|
| *m/e* | Intensity, chart div. | *m/e* | Intensity, chart div. |
| 12 | 530 | 24 | 670 |
| 13 | 1500 | 25 | 2230 |
| 14 | 3580 | 26 | 17600 |
| 15 | 33700 | 27 | 22500 |
| 16 | 39400 | 28 | 37200 |
| 17 | 1780 | 29 | 1250 |
| 26 | 58 | 37 | 8 |
| 27 | 167 | 38 | 20 |
| 28 | 163 | 39 | 190 |
| 29 | 990 | 40 | 17 |
| 30 | 30 | 41 | 830 |
| | | 42 | 24 |
| | | 50 | 26 |
| | | 51 | 33 |
| | | 52 | 14 |
| | | 53 | 102 |
| | | 54 | 6 |
| | | 55 | 72 |

(11) When discrepancies appear between this paper and a previous note (THIS JOURNAL, **78**, 5697 (1956)), the present results supersede the earlier ones.

TABLE II

APPEARANCE POTENTIALS AND REACTIONS

| m/e | $A_1$ (e.v.) | Probable process | $A_2$ (e.v.) | Probable process |
|---|---|---|---|---|
| | | Ions from methane | | |
| 17 | 10.9 | $CH_4 + N_2 \rightarrow NH_3^+ \ldots$<br>$NH_3 \rightarrow NH_2^+ (I = 10.5^a)$ ? | 12.8 | $CH_4 \rightarrow CH_4^+$<br>$CH_4^+ + CH_4 \rightarrow CH_5^+ + CH_3$[b] |
| 26 | 11.5 | $2CH_4 \rightarrow C_2H_2 + 2H_2$<br>$C_2H_2 \rightarrow C_2H_2^+ (I = 11.4)$ | | |
| 27 | 12.1 | ? | | |
| 28 | 11.4 | ? | | |
| 29 | 12.6 | ? | 13.9 | $CH_4 \rightarrow CH_3^+ + H$ ($A = 14.4$)<br>$CH_3^+ + CH_4 \rightarrow C_2H_5^+ + H_2$,[c]<br>$\Delta H = -19$[d] |
| | | Ions from ethylene | | |
| 24 | 11.7 | $C_2H_4 \rightarrow C_2 + 2H_2$<br>$C_2 \rightarrow C_2^+ (I = 11.5)$ | | |
| 26 | 11.4 | $C_2H_4 \rightarrow C_2H_2 + H_2$<br>$C_2H_2 \rightarrow C_2H_2^+ (I = 11.4)$ | 12.9 | $C_2H_4 \rightarrow C_2H_2^+ + H_2$<br>($A = 13.5$) |
| 28 | 10.3 | $C_2H_4 \rightarrow C_2H_4^+ (I = 10.6)$ | | |
| 29 | .. | $C_2H_3^+ + C_2H_4 \rightarrow C_2H_5^+ + C_2H_2$,[c] $\Delta H = -16$ | | |
| 39 | 11.8 | $C_2H_4 \rightarrow C_2H_2 + H_2$<br>$C_2H_2 \rightarrow C_2H_2^+ (I = 11.4)$<br>$C_2H_2^+ + C_2H_4 \rightarrow C_3H_3^+ + CH_3$, $\Delta H = -15$ | 13.8 | $C_2H_4 \rightarrow C_2H_2^+ + H_2$ ($A = 13.5$)<br>$C_2H_2^+ + C_2H_4 \rightarrow C_3H_3^+ + CH_3$,[c]<br>$\Delta H = -15$ |
| 41 | 10.1 | $C_2H_4 \rightarrow C_2H_4^+ (I = 10.6)$<br>$C_2H_4^+ + C_2H_4 \rightarrow C_3H_5^+ + CH_3$,[c] $\Delta H = -17$ | | |
| 50 | 24.5 | $C_2H_4 \rightarrow C_2^+ + H_2 + H(?)$ ($A = 26.5$)<br>$C_2^+ + C_2H_4 \rightarrow C_4H_2^+ + H_2$, ($\Delta H = -162$) | | |
| 51 | 19.5 | $C_2H_4 \rightarrow C_2H^+ + H_2 + H$ ($A = 19.3$)<br>$C_2H^+ + C_2H_4 \rightarrow C_4H_3^+ + H_2$, $\Delta H = -92$ | | |
| 53 | 12.7 | $C_2H_4 \rightarrow C_2H_2^+ + H_2$ ($A = 13.5$)<br>$C_2H_2^+ + C_2H_4 \rightarrow C_4H_5^+ + H$, $\Delta H = -13(?)$ | | |
| 55 | 10.8 | $C_2H_4 \rightarrow C_2H_4^+ (I = 10.6)$<br>$C_2H_4^+ + C_2H_4 \rightarrow C_4H_7^+ + H$, $\Delta H = -15$ | | |

[a] Ionization potentials ($I$) and appearance potentials ($A$) in e.v. Values taken from tabulation given in reference 2. [b] Reaction previously observed by Tal'roze and Lyubimova, reference 3. [c] Reaction previously observed by Schissler and Stevenson, reference 5. [d] Heats of reaction in kcal./mole. Values are calculated from ionic heats of formation tabulated in reference 2.

reactions by which they are formed. $A_1$ and $A_2$ refer to the lower and higher critical potentials found in a given ionization efficiency curve. The identification of the reactant ions has been made by considering the energetics of possible reactions, the appearance potentials of the various ions, and the dependence of the ion abundance upon pressure and repeller voltage. All the reactions involving the gas phase reactions of ions show second-order pressure dependence, and their repeller voltage dependence corresponds to that of a secondary ion. The accepted values of the primary ion ionization and appearance potentials with which the secondary ion appearance potentials are to be compared are given parenthetically in Table II. It is assumed that only exothermic secondary reactions will be observed, and this assumption can be justified by detailed considerations. The heats for the secondary reactions thought to occur are given in Table II.

**Additional Comments on Table II:** $m/e = 24$ and 26 from $C_2H_4$.—The appearance potentials of these ions were determined to learn the technique of making appearance potential measurements at high pressures. The ethylene mass 28 ion was used to calibrate the ionizing voltage scale. The two high pressure critical potentials observed for the mass 26 ion agree closely with the accepted values for the ionization potential of $C_2H_2$ and the appearance potential for the electron impact process $C_2H_4 \rightarrow C_2H_2^+ + H_2$, respectively; and this agreement indicates strongly that the lower high pressure value refers to acetylene molecules formed by pyrolysis from ethylene. Similarly, since the appearance potential for the formation of mass 24 ion from ethylene by fragmentation under electron impact is 26.5 volts,[2] the high pressure appearance potential for this ion refers to $C_2$ formed by pyrolysis and really constitutes a measure of the ionization potential of the $C_2$ molecule. As such it confirms the value of $I(C_2) = 11.5 \pm 1.0$ volts found by Chupka and Inghram.[12] By contrast, we found no evidence that products of mass 25 or 27 are produced in the pyrolysis of ethylene.

$m/e = 39$ from $C_2H_4$.—Two appearance potentials of $C_3H_3^+$ were found, the lower one corresponding to, although slightly greater than, $I(C_2H_2)$, and the upper falling midway between $A(C_2H_2^+)$ and

(12) W. A. Chupka and M. G. Inghram, *J. Chem. Phys.*, **21**, 371 (1953).

$A(C_2H_3^+)$. Because of this uncertainty, the $C_3H_3^+$ abundance was studied with a small, fixed concentration of ethylene and various concentrations of acetylene. The $C_3H_3^+$ abundance was linear with the acetylene concentration, and we conclude that this ion is formed from $C_2H_2^+$.

$m/e = 29$ from $C_2H_4$.—This peak in part is attributable to $C^{12}C^{13}H_4^+$. Its dependence upon repeller voltage was different from that of any other ion we have observed in that the total abundance of $m/e = 29$ decreased to that of $C^{12}C^{13}H_4^+$ (and even considerably lower) when the repeller voltage gradient increased above about 25 volt/cm. In view of this peculiar behavior no appearance potential was determined, but the only reasonable reaction is $C_2H_3^+ + C_2H_4 \rightarrow C_2H_5^+ + C_2H_2$, $\Delta H = -16$ kcal./mole.

**Experimental Reaction Rate Constants.**—From equation 5 it is seen that the slope of the linear portion of the plot of $I_S/(I_P + I_S)$ *vs.* ionization chamber molecular concentration is equal to $(k_{s_i^+}/\sum_j k_{s_j^+})k_1 \tau_{P^+}$, and using values of $\tau_{P^+}$ calculated from equation 7b, $(k_{s_i^+}/\sum_j k_{s_j^+})\, k_1$ is readily obtained. When only one product ion is formed from a given transition state ion $(k_{S_i^+}/\sum_j k_{s_j^+})k_1$ reduces to $k_1$, the bimolecular rate constant. When several product ions are formed $k_1$ is obtained by taking $\sum_j (k_{s_i^+}/\sum_j k_{s_j^+})k_1$. Table III contains the rate constants for all the reactions of methane and ethylene subjected to pressure studies. In these measurements the repeller voltage was kept at 1.0 volts.

TABLE III

RATE CONSTANTS FROM PRESSURE STUDIES ($V_R$ = 1.0 VOLT)

| Reaction | $(k_{s_i^+}/\Sigma_j k_{s_j^+})k_1 \times 10^{10}$ (cc./molecule sec.) | | $k_1 \times 10^{10}$ (cc./molecule sec.) |
|---|---|---|---|
| | 8.9 | | |
| $CH_4^+ + CH_4 \rightarrow CH_5^+ + CH_3$ | 9.4 | 8.93 | 8.93 |
| | 8.5 | | |
| | 10.2 | | |
| $CH_3^+ + CH_4 \rightarrow C_2H_5^+ + H_2$ | 9.9 | 9.67 | 9.67 |
| | 8.9 | | |
| | 3.6 | | |
| $C_2H_3^+ + C_2H_4 \rightarrow C_2H_5^+ + C_2H_2$ | 3.8 | 3.82 | 3.82 |
| | 3.9 | | |
| | 4.0 | | |
| | 2.6 | | |
| $C_2H_2^+ + C_2H_4 \rightarrow C_3H_3^+ + CH_3$ | 2.4 | 2.50 | |
| | 1.6 | | |
| $C_2H_2^+ + C_2H_4 \rightarrow C_4H_5^+ + H$ | 1.6 | 1.60 | |
| $C_2H_2^+ + C_2H_4 \rightarrow (C_4H_6^+)$ | | | 4.10 |
| $C_2H_4^+ + C_2H_4 \rightarrow C_3H_5^+ + CH_3$ | 4.7 | 4.80 | |
| | 4.9 | | |
| $C_2H_4^+ + C_2H_4 \rightarrow C_4H_7^+ + H$ | 0.54 | 0.495 | |
| | 0.45 | | |
| $C_2H_4^+ + C_2H_4 \rightarrow (C_4H_8^+)$ | | | 6.30 |
| $C_2^+ + C_2H_4 \rightarrow C_4H_2^+ + H_2$ | 10.5 | 10.2 | 10.2 |
| | 9.8 | | |
| $C_2H^+ + C_2H_4 \rightarrow C_4H_3^+ + H_2$ | 4.7 | 5.8 | 5.8 |
| | 6.9 | | |

The percentage average deviations from average for replicate determinations of the rate constants for the eight reactions subjected to pressure studies ranged from 0 to 19%, with most of the deviations of the order 3–5%. We guess that an upper limit to the absolute uncertainty of the values is perhaps 15%.

When the pressure is held constant and the repeller voltage varied it is convenient to calculate the rate constant for each value of the voltage. Figure 5 is a typical curve showing the dependence

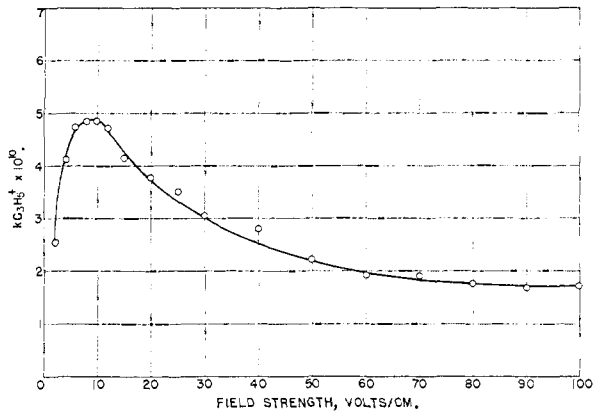


Fig. 5.—Rate constant for $C_2H_4^+ + C_2H_4 \longrightarrow C_3H_5^+ + CH_3$ against ion chamber field strength.

of the rate constant upon the ionization chamber electric field strength, and Table IV contains the rate constants at several field strengths, for all of the reactions subjected to repeller studies. The reservoir pressure was kept at 5 mm. The values tabulated are the averages of replicate measurements. As a matter of interest, measurements on the reaction $CH_4^+ + CH_4 \rightarrow CH_5^+ + CH_3$ were made at field strengths up to 220 volts/cm. The form of the curve up to a field strength of 100 volts/cm. was like that of Fig. 5, and above 100 volts/cm. the value of the rate constant remained essentially constant with a value of about $2.2 \times 10^{-10}$ cc./molecule sec.

The agreement between replicate determinations of the rate constants from repeller voltage studies (making comparisons at 10 volts/cm.) is generally satisfactory, the percentage deviations from average ranging from 1 to 15% with most of the deviations of the order of 5–10%. The agreement between the rate constant values determined from repeller studies (Table IV, 10 volt/cm. values) and pressure studies (Table III) is acceptable, the percentage differences between average values ranging from 0 to 15% for all values but one (42%) with most of the values falling between 0 and 10%.

It is interesting to note from Tables III and IV that the values of $k_1$ of all of the reactions differ from each other by at most about a factor of 2.5. These rate constants correspond to extremely fast reactions, and such fast reactions cannot have any appreciable energy of activation. This is in accordance with observations of Stevenson and Schissler[4] and of Schissler and Stevenson,[5] who measured

TABLE IV

REACTION RATE CONSTANTS AT VARIOUS FIELD STRENGTHS ($P_R \approx 5$ MM.)

| Reaction | $10^{10}(k_s^+j/\Sigma j k_s^+ j)k_1$, cc./molecule sec. at indicated $V/d$: 100 | 60 | 40 | 20 | 10 | 8 | 6 | 2 |
|---|---|---|---|---|---|---|---|---|
| $CH_4^+ + CH_4 \rightarrow CH_5^+ + CH_3$ | 2.2 | 4.8 | 7.0 | 8.4 | 8.5 | 8.5 | 8.0 | 5.0 |
| $CH_3^+ + CH_4 \rightarrow C_2H_5^+ + H_2$ | 3.4 | 5.4 | 7.4 | 8.8 | 8.4 | 7.8 | 7.0 | 4.8 |
| $C_2H_3^+ + C_2H_4 \rightarrow C_2H_5^+ + C_2H_2$[a] | | | | 0.9 | 3.0 | 3.2 | 3.4 | 2.2 |
| $C_2H_2^+ + C_2H_4 \rightarrow C_3H_3^+ + CH_3$ | 1.6 | 1.5 | 1.8 | 1.9 | 2.4 | 2.3 | 2.2 | 1.2 |
| $C_2H_2^+ + C_2H_4 \rightarrow C_4H_5^+ + H$ | 0.44 | 0.46 | 0.72 | 1.2 | 1.6 | 1.6 | 1.6 | 0.70 |
| $C_2H_2^+ + C_2H_4 \rightarrow (C_4H_6^+)$ | 2.0 | 2.0 | 2.5 | 3.1 | 4.0 | 3.9 | 3.8 | 1.9 |
| $C_2H_4^+ + C_2H_4 \rightarrow C_3H_5^+ + CH_3$ | 1.5 | 1.8 | 2.5 | 3.3 | 4.6 | 4.6 | 4.4 | 2.4 |
| $C_2H_4^+ + C_2H_4 \rightarrow C_4H_7^+ + H$ | 0.13 | 0.14 | 0.20 | 0.34 | 0.50 | 0.54 | 0.49 | 0.24 |
| $C_2H_4^+ + C_2H_4 \rightarrow (C_4H_8^+)$ | 1.6 | 1.9 | 2.7 | 3.6 | 5.1 | 5.1 | 4.9 | 2.6 |
| $C_2^+ + C_2H_4 \rightarrow C_4H_2^+ + H_2$ | 5.8 | 7.1 | 7.2 | 8.8 | 10.1 | 10.2 | 9.3 | 3.6 |
| $C_2H^+ + C_2H_4 \rightarrow C_4H_3^+ + H_2$ | 1.6 | 2.5 | 2.4 | 2.9 | 3.8 | 3.7 | 3.0 | 1.5 |

[a] Values very uncertain.

TABLE V

CROSS-SECTIONS, $\sigma$, IN CM.$^2$ $\times 10^{16}$ AT VARIOUS FIELD STRENGTHS

| Reaction | | 100 | 60 | 40 | 20 | 10 | 8 | 6 | 4 | 2 |
|---|---|---|---|---|---|---|---|---|---|---|
| $CH_4^+ + CH_4 \rightarrow CH_5^+ + CH_3$ | $f\sigma$ expt. | 5.6 | 15 | 27 | 45 | 61 | 66 | 68 | 71 | 55 |
| | $\sigma$ calcd. | 10 | 13 | 15 | 20 | 26 | 27 | 29 | 32 | 36 |
| $CH_3^+ + CH_4 \rightarrow C_2H_5^+ + H_2$ | $f\sigma$ expt. | 8.4 | 17 | 28 | 46 | 58 | 59 | 58 | 59 | 51 |
| | $\sigma$ calcd. | 10 | 13 | 15 | 20 | 26 | 27 | 29 | 32 | 36 |
| $C_2H_2^+ + C_2H_4 \rightarrow (C_4H_6^+) \rightarrow$ products | $f\sigma$ expt. | 6.4 | 8.2 | 12 | 21 | 36 | 38 | 41 | 40 | 27 |
| | $\sigma$ calcd. | 13 | 16 | 19 | 25 | 32 | 34 | 37 | 40 | 45 |
| $C_2H_4^+ + C_2H_4 \rightarrow (C_4H_8^+) \rightarrow$ products | $f\sigma$ expt. | 5.4 | 9.2 | 14 | 26 | 48 | 52 | 55 | 54 | 38 |
| | $\sigma$ calcd. | 13 | 16 | 19 | 25 | 32 | 34 | 37 | 40 | 45 |
| $C_2^+ + C_2H_4 \rightarrow C_4H_2^+ + H_2$ | $f\sigma$ expt. | 18 | 28 | 35 | 58 | 89 | 97 | 98 | 82 | 49 |
| | $\sigma$ calcd. | 13 | 16 | 19 | 25 | 32 | 34 | 37 | 40 | 45 |
| $C_2H^+ + C_2H_4 \rightarrow C_4H_3^+ + H_2$ | $f\sigma$ expt. | 5.1 | 10 | 12 | 19 | 34 | 36 | 32 | 29 | 21 |
| | $\sigma$ calcd. | 13 | 16 | 19 | 25 | 32 | 34 | 37 | 40 | 45 |

the rates of several such reactions at various temperatures. Unfortunately, we were unable to vary the temperature in our reaction zone. Stevenson and Schissler[4] have reported a value of $1.38 \times 10^{-9}$ cc./molecule sec. for the rate constant for the reaction $CD_4^+ + CD_4 \rightarrow CD_5^+ + CD_3$. The ionization chamber field strength is not stated. The agreement with our value for the reaction of $CH_4$ is good.

**Experimental Reaction Cross-sections.**—The reaction rates can be expressed in terms of reaction cross-sections, $f\sigma$. Experimental values of $f\sigma$ have been calculated from the current ratios using equation 8c taking $Q'$ values from equation 17, and these values (the averages of replicate determinations) are listed in Table V. Theoretical values of the cross-sections calculated from equation 29 described below are also listed in Table V. A graph of experimental and theoretical cross-sections against ionization chamber field strength is given in Fig. 6.

Schissler and Stevenson[5] report the following cross-sections

| Reaction | Cross-sections ($\times 10^{16}$) in cm.$^2$ at ion energy 0.10 e.v. | 1.00 e.v. |
|---|---|---|
| $CH_3^+ + CH_4 \rightarrow C_2H_5^+ + H_2$ | 165 ± 5 | 39 ± 1 |
| $C_2H_4^+ + C_2H_4 \rightarrow C_3H_5^+ + CH_3$ | 112 ± 3 | 21 ± 1 |
| $C_2H_2^+ + C_2H_4 \rightarrow C_3H_3^+ + CH_3$ | 24 ± 3 | 6 ± 1 |

The agreement with our experimental results (comparing Schissler and Stevenson's 0.10 and 1.00 e.v. values with our values at 4 and 40 volts/cm.) is not bad, particularly when it is remembered that the reactions to be compared are slightly different since we consider the total reactions for $C_2H_4^+$ and $C_2H_2^+$. Schissler and Stevenson[5] report that for the reactions tabulated the cross-sections decrease to zero at finite values of the average speed of the ion. We cannot deduce exactly how they calculate their average speed, and so we cannot make a definite comparison of our results with theirs. However, within the voltage range that we investigated, the cross-sections for all reactions but one remained finite. The exception is the formation of $C_2H_5^+$ from ethylene. Its behavior was very strange, and although we do not understand it, we are inclined to attribute it to unknown instrumental effects.

Our reaction cross-sections are quite large and relatively invariant from one reaction to another. By comparison, the gas kinetic cross sections of $CH_4$ and $C_2H_4$ at 423°K. are[13] $47.8 \times 10^{-16}$ cm.$^2$ and $66.5 \times 10^{-16}$ cm.$^2$, respectively.

**Theoretical Reaction Cross-sections.**—It is of interest to attempt to explain these large cross-sections theoretically. Following the general approach introduced by Eyring, Hirschfelder and Taylor,[14] we assume that the cross-section is determined by the distance, $r$, at which the centrifugal force tending to separate ion and molecule is exactly counterbalanced by the attractive force due

(13) Landolt-Börnstein Zahlenwerte and Functionen, 6 Auflage, "Atom und Molecularphysik," 1 Teil, Springer-Verlag, Berlin, 1950, p. 370.

(14) H. Eyring, J. O. Hirschfelder and H. S. Taylor, *J. Chem. Phys.*, **4**, 479 (1936). See also S. Glasstone, J. K. Laidler and H. Eyring, "The Theory of Rate Processes," McGraw-Hill Book Co., New York, N. Y., 1941, pp. 220 ff.

to polarization of the molecule by the ion. In our calculation it is assumed that all of the initial energy of the system (KE of ion and molecule and potential energy of the polarization interaction) is converted into rotational energy of the ion–molecule complex; we neglect any translational energy of the center of gravity of the complex. Thus, the theory is approximate, and cross-sections obtained from it constitute lower limits to the true values.

The rotation is treated classically. The centrifugal force away from center of mass must be the same for both ion and molecule, so

$$\frac{m_1v_1^2}{r_1} = \frac{m_2v_2^2}{r_2} \tag{21}$$

The center of mass of the system is defined by $m_1r_1 = m_2r_2$ with $r_1 + r_2 = r$, the distance between ion and molecule. From the definition of the center of mass, $r$, and equation 21

$$m_1v_1 = m_2v_2 \tag{22}$$

that is, the linear momentum of the molecule and ion must be equal when rotating. The energy must be conserved so

$$\frac{\alpha e^2}{2r^4} + T_1^0 + T_2^0 = T_1^f + T_2^f \tag{23}$$

where $T_1^0$ and $T_2^0$ are the initial average kinetic energy of the ion and molecule, respectively, $T_1^f$ and $T_2^f$ are the kinetic energies of the ionic and neutral components, respectively, of the transition state, and $\alpha$ is the polarizability of the molecule. From (22) and (23)

$$T_1^f = \frac{m_2}{m_1 + m_2}\left[\frac{\alpha e^2}{2r^4} + T_1^0 + T_2^0\right] \tag{24}$$

The average initial kinetic energies are

$$\bar{T}_1^0 = \left[\frac{eVd_0}{3} + \frac{3kT}{2}\right] \tag{25}$$

$$\bar{T}_2^0 = 3/2kT \tag{26}$$

In (25) and (26) $k$ is the Boltzmann constant, $T$ is the temperature, and the other terms are as defined previously. Combining equations 24, 25 and 26

$$T_1^f = \frac{m_2}{m_1 + m_2}\left[\frac{\alpha e^2}{2r^4} + 3kT + \frac{eVd_0}{3}\right] \tag{27}$$

The attractive force due to polarization is given by $2\alpha e^2/r^5$, and equating polarization force to centrifugal force

$$\frac{2\alpha e^2}{r^5} = \frac{2T_1^f}{r_1} \tag{28}$$

Substituting for $T_1^f$ and $r_1$ and taking $\sigma = \pi r^2$

$$\sigma = \frac{e\pi\sqrt{\alpha}}{\sqrt{6kT + \frac{2eVd_0}{3}}} \tag{29}$$

Theoretical cross-section values calculated from equation 29 are given in Table V and a plot is given in Fig. 6. The polarizability values used for $CH_4$ and $C_2H_4$ are $2.55 \times 10^{-24}$ cm.$^3$ and $4.06 \times 10^{-24}$ cm.$^3$, respectively, as calculated from molar polarization values given in Landolt–Börnstein.[15]

The theoretical and experimental cross-sections disagree at worst by about a factor of two, which is satisfactory for calculations of this kind. We conclude, then, that the theoretical treatment is for the most part valid and that the dominant factor in determining the cross-sections for these reactions is the ion–molecule polarization interaction. However, in addition to the disagreement in absolute values, theory and experiment do not agree well with respect to (1) the detailed functional dependence of the cross-sections upon ionization chamber field strength and (2) the fact that theory predicts that the cross-sections for the reactions of all ions with a given molecule will be the same, while in actuality some variation from one reaction to another does occur. While we are inclined to the belief that these disagreements result largely from inadequacies in the theory, some of the difficulty may result from experimental error and/or a variable experimental efficiency factor, $f$. In particular, we do not think that the maximum observed in the experimental $f\sigma$ *vs.* field strength relation at low field strengths is significant, but rather that it results from a lack of knowledge of the true conditions existing in the ionization chamber at low repeller voltages.

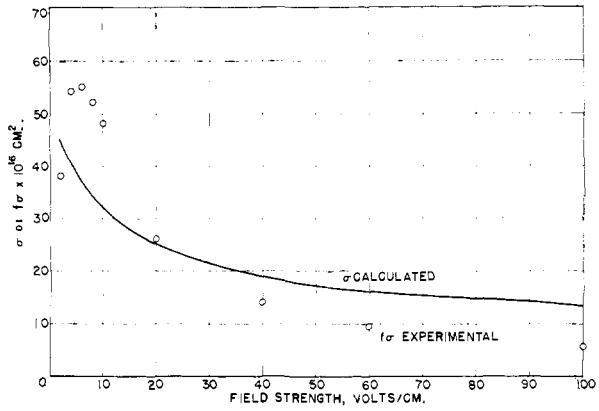


Fig. 6.—Cross-sections for $C_2H_4^+ + C_2H_4^+ \longrightarrow [C_4H_8^+]$.

Stevenson and Schissler[4] and Schissler and Stevenson[5] find a small negative temperature coefficient (for the cross-section ?) for some reactions, while for others the rate constant is independent of the temperature. It may be seen from equation 29 that the cross-sections theoretically should depend inversely on the temperature, and at low ionization chamber field strengths the cross-sections are approximately proportional to $T^{-1/2}$. From equations 5, 7b, 8c, 17 and 29 it may be seen that the dependence of the rate constant, $k_1$, on temperature will be very complicated and cannot be predicted. However, the theory cannot account for the occurrence of temperature coefficients in some reactions but not in others.

**Rate Constants for Thermal Speed Ions.**—We are not aware of the existence of any values based on experiment of bimolecular rate constants of gaseous thermal speed ions, and it is of considerable interest to attempt to get such values. We do not think that the rate constants we have obtained at zero repeller voltage correspond to thermal speed ions because of the previously discussed lack of definition of the potentials in the ionization chamber at very low voltages. Consequently, we prefer to obtain the rates by extrapola-

(15) Ref. 13, 3 Teil, p. 515.

tion from our more reliable higher field strength measurements.

For this purpose we require an extrapolation function which more adequately represents the field strength variation of the experimental $f\sigma$ values than does equation (29). As an empirical (but reasonable) procedure which is justified to the extent that it gives satisfactory results, we assume that $\sigma$ varies according to equation 29 and the efficiency factor, $f$, varies inversely with the velocity $p$, of the ion in the activated complex, *i.e.*, $f = \theta/p$ where $\theta$ is a proportionality constant. The kinetic energy of the ion in the complex is given by equation 27, from which $p$ is easily derived. Writing $r^4 = \sigma^2/\pi^2$ in the resulting expression for $p$ and taking $\sigma$ from equation 29, we obtain

$$f = \frac{1}{2}\left(\frac{m_1(m_1+m_2)}{m_2}\right)^{1/2}\frac{\theta}{(3kT+eVd_0/3)^{1/2}} \quad (30)$$

where the indices 1 and 2 refer to the ion and the molecule, respectively. Then $f\sigma$, the experimental cross-section, is

$$f\sigma = \frac{1}{2}\left(\frac{m_1(m_1+m_2)}{m_2}\right)^{1/2}\frac{\theta e\pi\alpha^{1/2}}{(3kT+eVd_0/3)} \quad (31)$$

The proportionality constant $\theta$ can be evaluated from one experimental value of $f\sigma$ or preferably from the slope of a plot of $f\sigma$ *vs.* $1/(3kT + eVd_0/3)$. The resulting function represents nicely the field strength variation of $f\sigma$ except for the dubious points at low field strengths, as is illustrated by the typical plot given in Fig. 7.

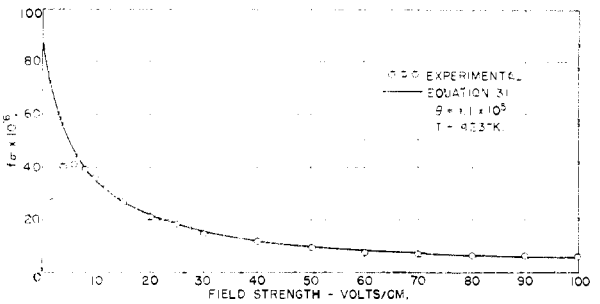


Fig. 7.—Typical plot of $f\sigma$ *vs.* field strength for $C_2H_2^+ + C_2H_4 \longrightarrow [C_4H_6^+]$.

The relationship between rate constant and cross-section is

$$k = f\sigma\bar{\xi} \quad (32)$$

where $\bar{\xi}$ is the relative velocity of the ion and molecule. Taking $f\sigma$ from equation 31 for $V = 0$ and $\bar{\xi}$ from equation 12 evaluated for thermal velocities, we obtain for the rate constant for thermal speed ions

$$k_{V=0} = \frac{\theta e}{6}\left(\frac{8\pi\alpha}{kT}\right)^{1/2}\left(\frac{m_\alpha+m_\beta}{m_\beta}\right)^{1/2} \quad (33)$$

The index $\alpha$ always refers to the lighter particle.

Eyring, Hirschfelder and Taylor[14] have developed an expression for the rate constant of thermal speed ions, namely

$$k = 2\pi\kappa\sigma\alpha^{1/2}\left(\frac{m_\alpha+m_\beta}{m_\alpha m_\beta}\right) \quad (34)$$

where $\kappa$ is the transmission coefficient. In Table VI we list thermal cross-sections and rate constants calculated by our extrapolation method and rate constants calculated from the Eyring, Hirschfelder and Taylor[14] expression taking $\kappa = 1$.

TABLE VI

CROSS-SECTIONS AND RATE CONSTANTS FOR THERMAL REACTIONS

| Reaction | Extrl. experimental $f\sigma_{298°K.}$ (cm.$^2$ × $10^{16}$) | Extrl. experimental $k_{298°K.}$ (cc./mole sec. × $10^9$) | Theoretical (EH&T) $k$ (cc./mole sec. × $10^9$) |
|---|---|---|---|
| $CH_4^+ + CH_4 \rightarrow CH_5^+ + CH_3$ | 221 | 2.8 | 1.3 |
| $CH_3^+ + CH_4 \rightarrow C_2H_5^+ + H_2$ | 251 | 3.2 | 1.3 |
| $C_2H_2^+ + C_2H_4 \rightarrow (C_4H_6^+)$ | 123 | 1.2 | 1.3 |
| $C_2H_4^+ + C_2H_4 \rightarrow (C_4H_8^+)$ | 155 | 1.5 | 1.3 |
| $C_2H^+ + C_2H_4 \rightarrow C_4H_3^+ + H_2$ | 131 | 1.2 | 1.3 |
| $C_2^+ + C_2H_4 \rightarrow C_4H_2^+ + H_2$ | 284 | 3.5 | 1.3 |

TABLE VII

COMPARISON OF PRIMARY AND SECONDARY MASS SPECTRA (BASED ON LARGEST OF THE PEAKS COMPARED)

| Ion | Primary 1-Butene | Primary *cis*-Butene-2 | Primary Isobutene | Primary Cyclobutane | Secondary from $C_2H_4^+ + C_2H_4$ |
|---|---|---|---|---|---|
| $C_3H_4^+$ | 6.5 | 7 | 11 | 6.5 | 1.5 |
| $C_3H_5^+$ | 100 | 100 | 100 | 100 | 100 |
| $C_4H_6^+$ | 2.5 | 4 | 2.5 | 3 | 0.2 |
| $C_4H_7^+$ | 18 | 22 | 16 | 21 | 8.8 |
| | 1,2-Butadiene | 1,3-Butadiene | 1-Butyne | 2-Butyne | From $C_2H_2^+ + C_2H_4$ |
| $C_3H_3^+$ | 100 | 100 | 100 | 57 | 100 |
| $C_4H_4^+$ | 28 | 11 | 10 | 23 | 7 |
| $C_4H_5^+$ | 100 | 59 | 57 | 100 | 54 |

With thermal rate constants and cross-sections of this magnitude it is self-evident that the occurrence of ionic reactions must be seriously considered in any process in which the formation of ions is a possibility, *e.g.*, in radiation chemistry processes. The agreement between our rate constants and those from Eyring, Hirschfelder and Taylor[14] is satisfactory, but it should be noted that our treatment predicts a weak ($T^{-1/2}$) dependence of the rate constant on temperature, which is not found in the EH&T expression. We do not know which of these predictions is correct.

**Comparison of Secondary and Primary Mass Spectra.**—In those cases where a known intermediate such as $C_4H_8^+$ or $C_4H_6^+$ is formed it is interesting to compare the primary mass spectrum from various $C_4H_8$ and $C_4H_6$ compounds with our observed secondary spectrum. Thus the intensities of those peaks in the secondary mass spectrum of ethylene which might have resulted from the reaction of $C_2H_4^+$ and $C_2H_4$ are compared to those of the same peaks in the primary spectra of various $C_4H_8$ compounds. Similarly the secondary spectra that might have resulted from the reaction of $C_2H_2^+$ and ethylene are compared to those of several $C_4H_6$ compounds. Such comparisons are made in Table VII taking the primary spectra from the API tabulation. There is an approximate correspondence which indicates that the intermediate ions (activated complex) must be at least qualitatively similar to the respective parent ions in the

primary spectra. In fact, it is tempting to decide that the $C_4H_6^+$ intermediate is more similar to the 1,3-butadiene or 1-butyne ions than to the other two primaries shown.

**Acknowledgment.**—We wish to express our appreciation to Mr. Burl L. Clark for his invaluable help in making the measurements and calculations.

BAYTOWN, TEXAS

---

[CONTRIBUTION FROM THE DEPARTMENT OF CHEMISTRY OF THE UNIVERSITY OF WISCONSIN]

# Effects of Structure, Product Concentration, Oxygen, Temperature and Phase on the Radiolysis of Alkyl Iodides

BY EVALYN O. HORNIG AND JOHN E. WILLARD

RECEIVED DECEMBER 20, 1956

The yields of elemental iodine as a function of radiation dosage have been determined for the radiolysis with $Co^{60}$ $\gamma$-rays of seven purified degassed alkyl iodides. Doses $>16 \times 10^{20}$ e.v./ml. were used in some cases. Although six of the iodides show linear dependence of $G_{I_2}$ on radiation dosage at low doses, all depart from linearity at higher doses, and the $G_{I_2}$ for isobutyl iodide decreases with increasing dose even at the start of irradiation. The linear dependence is attributed to a balanced competition between HI and $I_2$ for thermal radicals and, consistent with this concept, the rate of exchange with radioiodine during radiolysis is found to be dependent on the concentration of added $I_2$ or $O_2$. The dependence of $G_{I_2}$ on the $\beta$-hydrogen content of the alkyl iodides is confirmed and ascribed to increased probability of HI formation by decomposition of excited molecules as the number of $\beta$-hydrogens per molecule increases. Added $O_2$ increases the initial $G_{I_2}$ for $C_2H_5I$ by an amount independent of the $O_2$ pressure from 2 to 188 mm., but as the $I_2$ concentration increases with increased dosage $G_{I_2}$ returns to its degassed level at a rate inversely dependent on the oxygen pressure. With added iodine present at a concentration elevenfold greater than the dissolved oxygen, the initial $G_{I_2}$ was the same as that in the absence of additives. $G_{I_2}$ for four iodides tested is essentially independent of temperature in the liquid phase from 20 to $-78°$ and for $C_2H_5I$ from 108 to $-78°$, but the $G_{I_2}$ values for both $CH_3I$ and $C_2H_5I$ have a positive temperature coefficient in the crystalline solid phase. $G$ values for two iodides studied in both the glassy and crystalline states at $-190°$ were higher in the glassy state, a result which is tentatively ascribed to molecular orientation favoring a stereospecificity for hot radical reactions.

## Introduction

The purpose of the work of this and the following paper[1] was to elucidate further[2] the mechanisms of radiolysis of the alkyl iodides. The investigations have included studies of: (1) the competitive reactions of $O_2$, $I_2$ and HI with thermal radicals produced in the radiolyses and (2) the effects of temperature, molecular structure and irradiation in the solid crystalline and glassy states on the yields of elemental iodine.

## Experimental

The alkyl iodides, Eastman or Matheson best grade, were purified by passage through activated alumina, followed by distillation through a two-foot Vigreux column, the middle 50% being retained. Identical iodine yields were obtained from the irradiation of samples of ethyl iodide purified as above, and from those purified by shaking with concentrated $H_2SO_4$ and washing with $Na_2SO_3$ solution prior to distillation. The purified iodides were degassed by several cycles of freezing, pumping and thawing on a vacuum system, and then were vacuum-distilled through $P_2O_5$ into the irradiation vessels and sealed off.

During the irradiation, the samples (5 ml.) were contained in an annular vessel,[4] which surrounded a 40-curie $Co^{60}$ $\gamma$-ray source.[4] The radiation intensity on the samples was $2 \times 10^5$ roentgens/hr., the absorption of energy in the alkyl iodides being at the rate of about $2 \times 10^{19}$ e.v. per ml. per hr.

Iodine analyses were made with a Beckman DU spectrophotometer. A spectrophotometer cell made from square Pyrex tubing was attached to the annular vessel so that iodine analyses could be made between successive irradiations of the same sample without exposing it to the air. Concentrations were read at the absorption maximum at 478 m$\mu$ and for high concentrations at 550 and 625 m$\mu$. The high concentration readings were checked at 478 m$\mu$ in methyl and ethyl iodide irradiations by using 0.98 and 0.95 cm. silica inserts in the analysis cells. Determinations of molar extinction coefficients were made at the three wave lengths for methyl, ethyl and *n*-propyl iodides, the values obtained being 1280, 356 and 72.8 l./mole cm., respectively. Since the extinction coefficients were the same for the three iodides, it was assumed that the same values would also be applicable to the other iodides.

To irradiate samples at $-78$, $-123$ and $-190°$, they were surrounded during the irradiation by baths of solid $CO_2$ and acetone, butyl chloride slush, and liquid air, respectively. A thermostatically controlled bath of mineral oil was used for the irradiations at 108°.

Oxygen of known pressure was admitted to degassed samples of ethyl iodide on a vacuum line, either from a cylinder or by heating $KClO_3$ containing $MnO_2$. The number of moles oxygen introduced to the sample vessel was determined from the pressure change in a known volume of the vacuum apparatus, measured with a phosphoric acid manometer. The solubility of oxygen in ethyl iodide was found to be $8 \times 10^{-6}$ mole/l. per mm. pressure at 23°,[5] so that the concentration of dissolved oxygen in the samples could be determined from the gas pressure.

Iodine labeled with $I^{131}$ was prepared from carrier-free iodine solutions by adding the desired amount of KI and oxidizing with acidified $KIO_3$. The iodine was transferred into the irradiation vessels by vacuum distillation through $P_2O_5$. A solution-type Geiger counter was used to measure

(1) R. J. Hanrahan and J. E. Willard, THIS JOURNAL, **79**, 2434 (1957).

(2) Previous investigators have determined the relative yields of $I_2$ from X-ray and $\alpha$-particle irradiation of air-saturated ethyl iodide,[3a] from $\gamma$-irradiation of eight air-saturated alkyl iodide,[3b] from fast electron irradiation[3c] of degassed $CH_3I$, $CH_2I_2$, $C_2H_5I$ and *n*-$C_3H_7I$, and from X-ray irradiation of degassed $CH_3I$,[3c,d] $C_2H_5I$,[3c,d,h] propyl[3d,h] and butyl iodides.[3d] The yields of various products from the X-ray irradiation[3e,h] and very low intensity $Co^{60}$ $\gamma$-ray irradiation[3g] of degassed $CH_3I$ have also been determined. Similarities and contrasts between the radiolysis and photolysis of the alkyl iodides have been considered.[3c,d,e,f] Distillation with added carriers following irradiation in the presence of radioiodine has been used to identify intermediate free radicals.[3g,h]

(3) (a) M. Lefort, P. Bonet-Maury and M. Frilley, *Compt. rend.*, **226**, 1904 (1948); (b) P. Sue and E. Saeland, *Bull. soc. chim. France*, 437 (1949); (c) R. H. Schuler and W. H. Hamill, THIS JOURNAL, **74**, 6171 (1952); (d) E. L. Cochran, W. H. Hamill and R. R. Williams, Jr., *ibid.*, **76**, 2145 (1954); (e) C. R. Petry and R. H. Schuler, *ibid.*, **75**, 3796 (1953); (f) W. H. Hamill and R. H. Schuler, *ibid.*, **73**, 3466 (1951); (g) L. H. Gevantman and R. R. Williams, Jr., *J. Phys. Chem.*, **56**, 569 (1952); (h) R. H. Schuler and R. C. Petry, THIS JOURNAL, **78**, 3957 (1956).

(4) R. F. Firestone and J. E. Willard, *Rev. Sci. Inst.*, **24**, 904 (1953).

(5) E. O. Hornig, Ph.D. thesis, University of Wisconsin, Feb. 1956, available from University Microfilms, Ann Arbor, Michigan.